Transport mechanism of spray pyrolyticgrown indium tin oxide/indium phosphide junctions

V. Vasu, P. Manivannan, and A. Subrahmanyam

Citation: Journal of Applied Physics **77**, 5220 (1995); doi: 10.1063/1.359271
View online: http://dx.doi.org/10.1063/1.359271
View Table of Contents: http://scitation.aip.org/content/aip/journal/jap/77/10?ver=pdfcov
Published by the AIP Publishing

Transport mechanism of spray pyrolytic-grown indium tin oxide/indium phosphide junctions

V. Vasu, P. Manivannan, and A. Subrahmanyam[a)]
Semiconductor Laboratory, Department of Physics, Indian Institute of Technology, Madras-600 036, India

(Received 25 July 1994; accepted for publication 24 January 1995)

Indium tin oxide (ITO)/*p*-indium phosphide (InP) junctions have been prepared by the spray pyrolysis technique and the photovoltaic properties have been reported earlier. Continuing our efforts to understand the transport mechanism across these junctions, XPS, current-voltage (dark), and capacitance-voltage measurements have been carried out on the samples having 10.2% photovoltaic efficiency under 100 mW/cm^2 illumination. The XPS studies have confirmed an interfacial layer consisting of In_2O_3 and $InPO_4$. The transport mechanism above 300 K is found to be dominated by recombination at the depletion region. The MIS model proposed in our earlier paper to account for the photovoltaic and transport properties is confirmed for sprayed ITO/*p*-InP junctions in the present study. © *1995 American Institute of Physics.*

I. INTRODUCTION

Indium phosphide (InP) solar cells are very attractive because of their high efficiency[1] and superior radiation resistance.[2,3] The structure of indium tin oxide (ITO)/InP, in view of ease of preparation, have attracted the attention of several groups.[4–9] Various techniques have been employed to prepare these cells; however, very few reports are available on spray pyrolysis, a technique viable for large scale applications. In our earlier papers[10,11] the effect of substrate temperature and tin doping on the photovoltaic properties of sprayed In_2O_3/*p*-InP junctions have been reported. A maximum efficiency of 10.2% (under 100 mW/cm^2 illumination) has been observed for the junctions prepared at 340 °C with a tin concentration of 5% by weight. We have proposed the metal-insulator-semiconductor (MIS) model to explain the observed photovoltaic properties; it is conjectured that a semi-insulating In_2O_{3-x} is the interfacial layer. It may be mentioned here that the only other available report on ITO/*p*-InP solar cells prepared by spray technique[12] has suggested a homoburied junction.

In continuation of our efforts, more details of the interfacial layer are studied by x-ray photoelectron spectroscopy. Also capacitance-voltage (*C-V*) measurements and temperature variation of dark current-voltage (*I-V*) measurements are reported in the present paper to understand the transport mechanism across the junction.

The dark *I-V* and *C-V* measurements have been carried out on ITO/*p*-InP junctions having an efficiency of 10.2%.[10,11] The experimental methods to prepare these ITO/*p*-InP junctions along with the details of measurement techniques have been described earlier.[6,10,11]

II. RESULTS AND DISCUSSION

In the following sections, the XPS studies, dark *I-V* characteristics measured over a temperature range 200–370 K and *C-V* measurements on ITO/*p*-InP junctions prepared by spray pyrolysis at 340 °C with 5% by weight of tin in ITO films are reported. The *p*-InP wafers employed are Zn doped, (111) oriented, having a carrier density 10^{17} cm^{-3} and are single side polished.

A. XPS studies

A thin ITO film (~100 Å) is deposited on a *p*-InP wafer under nearly identical conditions as mentioned for those samples which have shown an efficiency of 10.2%: 340 °C, 5% tin by weight in ITO films. The XPS studies have been carried out using a ESCALAB Mark II instrument (VG Scientific Ltd., UK) equipped with Mg K_α x rays (1253.6 eV) and argon ion sputtering facilities. The ITO/*p*-InP interface is probed by progressive etching on junctions for 5, 10, and 20 min, respectively.

The identification of elements/compounds at the ITO/*p*-InP interface in the present study has been done by using the core level binding energy shift data and comparison with published results for standard compounds. Figures 1(a) and 1(b) show the signatures of In:3*d* and O:1*s* core level spectra of ITO/*p*-InP junctions before and after progressive argon ion etching. The In:3*d* peak observed at 444.7 eV for the as-prepared sample [Fig. 1(a)] corresponds to In_2O_3.

After etching for 5 min, an additional shoulder has been observed in the In:3*d* peak. A Gaussian/Lorentzian curve fitting algorithm was used to deconvolute multiple component peaks. Figure 2(a) shows the deconvoluted peaks at 444.0 and 446.0 eV corresponding to InP and $InPO_4$ (Ref. 13), respectively. It may be mentioned here that the peak corresponding to P:2*p* for $InPO_4$ could not be observed, due to the low ionization cross section of phosphorus. Since the energy separation between the In:3*d* peak for In_2O_3 and $InPO_4$ is nearly 2 eV, it may be reasonable to attribute the high-energy shoulder of In:3*d* to a complex of $InPO_4$.

The O:1*s* peak is observed [Fig. 1(b)] at 532 eV for all the cases (except for 20 min etching). The literature values[13] indicate that this peak corresponds to InP_xO_y. The deconvoluted O:1*s* spectra [Fig. 2(b)] shows peaks at 530.5 and 532.1 eV corresponding to In_3O_3 and $InPO_4$, respectively. These binding energy values are in good agreement with the values reported.[13–15] It should be mentioned here that peaks of oxygen bonded in In_2O_3 and $InPO_4$ are so close

a)Electronic mail: phy3@iitm.ernet.in

 0021-8979/95/77(10)/5220/5/$6.00

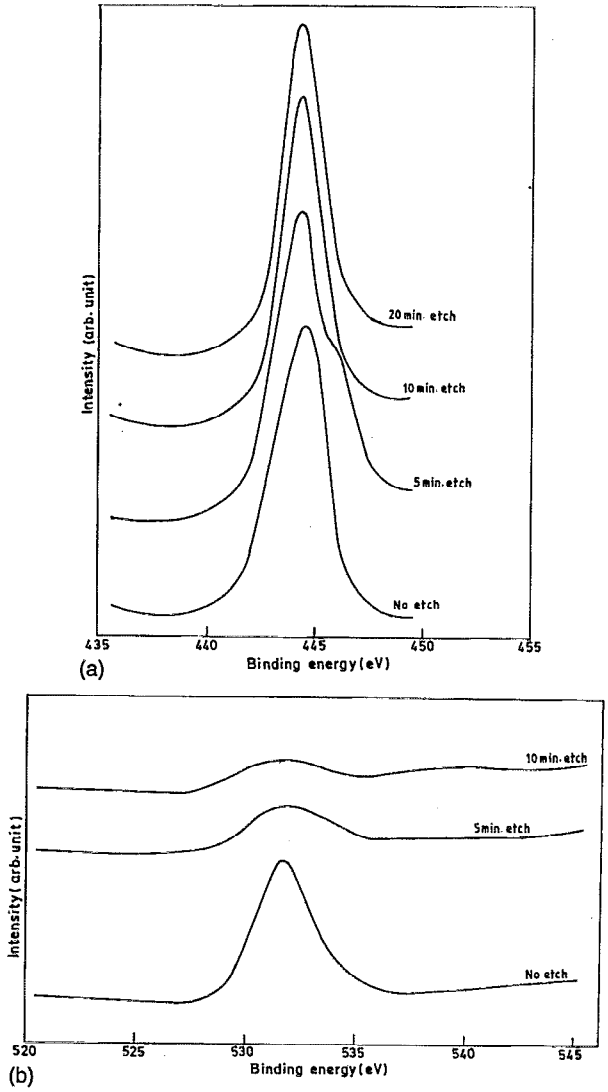

FIG. 1. (a) XPS In:3d spectra for ITO/p-InP junction at different argon ion etches. (b) XPS O:1s spectra for ITO/p-InP junction at different argon ion etches.

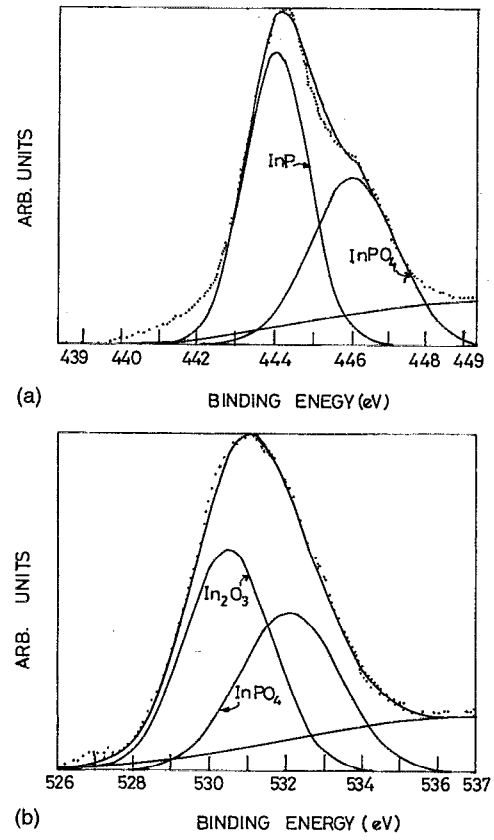

FIG. 2. (a) XPS In:3d spectra for 5 min argon ion etch of thin ITO/p-InP. Deconvoluted peaks correspond to In_2O_3 and $InPO_4$. Linear background is also shown. (b) XPS O:1s spectra for 5 min argon ion etch of thin ITO/p-InP. Deconvoluted peaks correspond to In_2O_3 and $InPO_4$. Linear background is also shown.

in terms of energy, it is extremely difficult to identify the compound using the O:1s peak.[16]

The energy separation between the deconvoluted peaks of In:3d and O:1s at lower energies clearly confirm the presence of In_2O_3.

From these results, it may be inferred that there exists a thin interfacial layer consisting mixture of In_2O_3 and $InPO_4$, however, it is not possible to estimate the thickness of the interfacial layer from the XPS studies. This interfacial layer is formed during the preparation of the ITO/p-InP junction. It may be recalled that the spray pyrolysis technique involves preheating of the substrate (InP) to 340 °C under atmospheric conditions; it is very likely that the InP surface exposed can interact with the oxygen available in the reaction chamber resulting in substoichimetric oxides of indium and phosphorous. It is not possible to identify precisely the substoichiometry of the interfacial $InPO_4$ and In_2O_3 in the present investigation.

As a pausing comment it may be mentioned here that the presence of Cl is observed at 199 eV for as-prepared ITO/p-InP junctions (Fig. 3), the intensity of the chlorine peak almost vanishes at the 10 min etch. It is generally believed that spray pryolytic-grown interfaces do contain Cl contamination. However, the details of the defect levels introduced by chlorine impurity and its effect on the transport mechanism need a more detailed study and it is beyond the scope of the present paper.

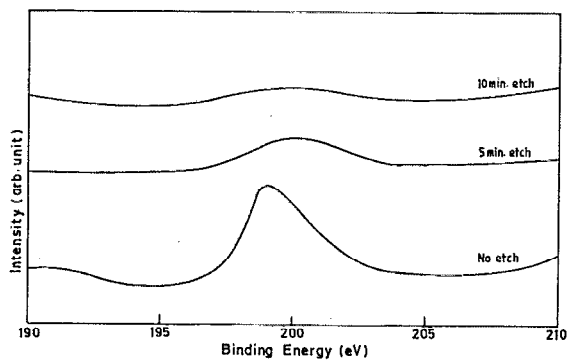

FIG. 3. XPS Cl:2p spectra for ITO/p-InP junction at different argon ion etches.

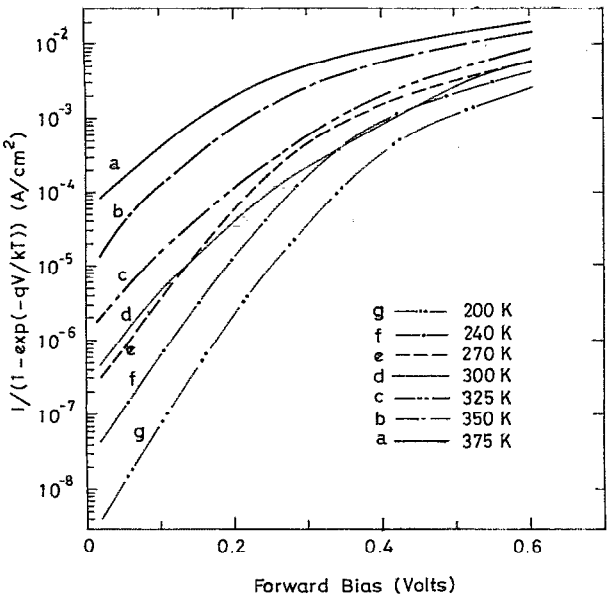

FIG. 4. Dark forward I-V characteristics of ITO/p-InP junction with temperature as variable.

B. Dark I-V characteristics

The dark current-voltage (I-V) measurements over a temperature range of 200–375 K have been made on the ITO/p-InP cells which have shown to 10.2% photoconversion efficiency.[10,11] A cryostat has been designed and fabricated for the measurements. The measured temperature has a maximum error of ± 1 K.

Since the interfacial layer between ITO and InP (consisting of $InPO_4$ and In_2O_3) is confirmed, the following section assumes the Schottky barrier model with an interfacial layer.

For an evaluation of the transport mechanism, one needs the values of n (diode ideality factor), J_0 (reverse saturation current density), A^* (the Richardson constant), ϕ_b (barrier height), and E_a (activation energy). The following section derives these parameters for spray pyrolytic ITO/p-InP junctions.

The forward I-V characteristics for an ideal Schottky diode, when the barrier height is dependent on the applied bias, may be is written as[17]

$$J=J_0 \exp\left(\frac{qV_f}{nkT}\right)\left[1-\exp\left(-\frac{qV_f}{kT}\right)\right], \tag{1}$$

where J_0 is the reverse saturation current density, n the diode ideality factor, V_f is the forward bias, k the Boltzmann constant, and T is the temperature in K (at which measurement has been made). The above equation is valid for $V_f<3kT/q$ and even for reverse bias. Figure 4 shows the $\ln(J)/[1-\exp(qV_f/kT)]$ vs V_f plot at different temperatures under forward bias condition. The values of n and J_0 have been calculated from the slope and intercept of the straight line portion of the I-V plot, respectively.

It may be observed (Table I) that with increasing temperature, J_0 increases and n shows very little variation.

Following the Richardson's equation

TABLE I. The diode ideality factor and the reverse saturation current as a function of temperature.

Temperature (K)	Ideality factor 'n'	Reverse saturation current J_0 (A/cm^2)
200	1.63	2.1×10^{-9}
240	1.53	2.7×10^{-8}
270	1.49	2.0×10^{-7}
300	1.62	4.1×10^{-7}
325	1.64	1.7×10^{-6}
350	1.58	1.4×10^{-5}
375	1.64	6.5×10^{-5}

$$J_0=A^*T^2 \exp\left(-\frac{\phi_b}{kT}\right) \tag{2}$$

(where ϕ_b is the effective barrier height and A^* is the effective Richardson constant), $\ln(J_0/T^2)$ is plotted against $1/T$ in Fig. 5. As is well known, the slope and the y intercept of the Richardson plot gives the barrier height and the Richardson constant, respectively. From Fig. 5, it may be seen that the curve clearly exhibits two slopes: 0.61 eV above 270 K, and 0.24 eV below 300 K. The corresponding Richardson constants are 0.07 and 6×10^{-8} A/cm^2/K, respectively. These features clearly indicate two distinct transport mechanisms at different temperatures. The barrier height of 0.61 eV (above 270 K) corresponds closely to the observed open circuit voltage; however, the Richardson constant is lower by two orders of magnitude in comparison to the available literature value.[18] Such a low A^* value, in general, is attributed to the presence of an interfacial layer. The existence of such an interfacial layer in the present study has already been confirmed by XPS studies.

In order to evaluate the activation energy for the transport process, J_0 is plotted against the inverse of temperature

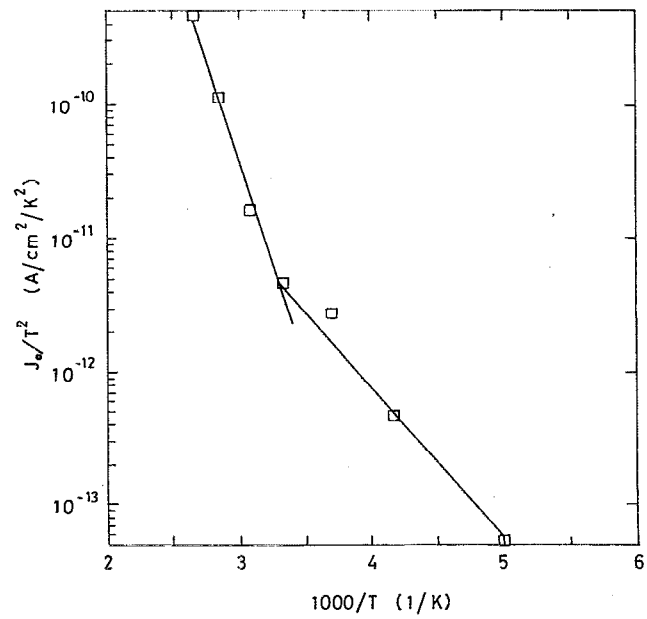

FIG. 5. Richardson plot for ITO/p-InP junction.

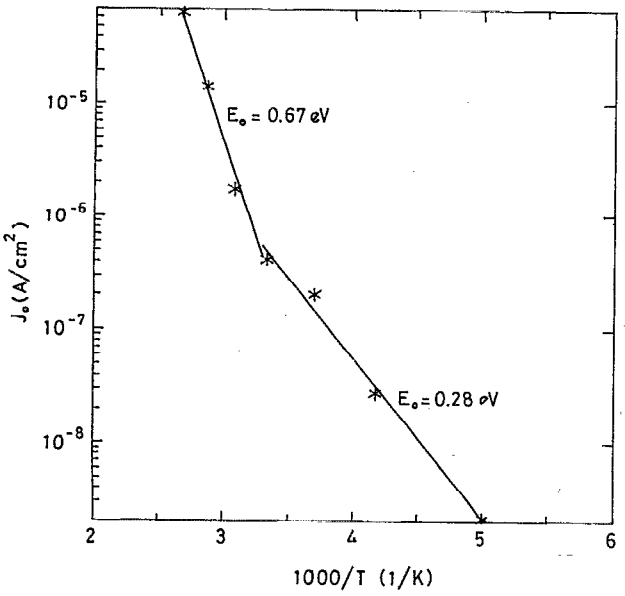

FIG. 6. Reverse saturation current plotted against inverse of temperature for ITO/p-InP junction.

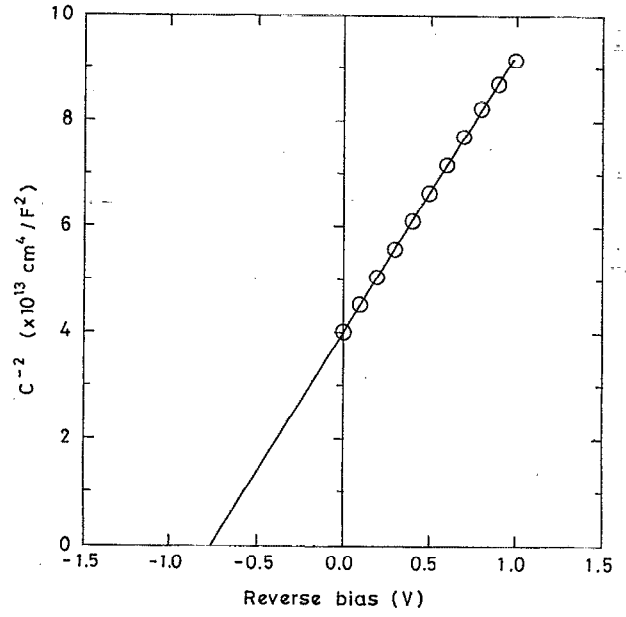

FIG. 7. $1/C^2$ vs reverse bias voltage plot for ITO/p-InP junction.

(Fig. 6) for ITO/p-InP junctions; two slopes with activation energies 0.67 and 0.28 eV above and below 270 K, respectively, are observed. Similar results have been obtained by Yu and Snow[19] on Pt-Si Schottky diodes and Wolf *et al.*,[20] on proton irradiated silicon solar cells. Earlier observations and analyses have shown that if the activation energy (E_a) is compared to the band gap (E_g) of the base semiconductor, the transport process may be identified; for example, if E_a is approximately equal to $E_g/2$, it is a recombination process, if $E_a \sim E_g$ thermionic emission dominates, and if $E_a > E_g/2$ it is field emission process.

In the present case, above 270 K, the activation energy close to the half the band gap of InP indicates that recombination at the depletion region is the dominant transport mechanism.

As is well known, the recombination current at the depletion region follows the relation[20]

$$J_0 \propto T^{3/2} \exp\left(-\frac{(E_g/2)+E_t-E_i}{kT}\right), \tag{3}$$

where E_t is the trap energy and E_i is the intrinsic band gap. From Eq. (3), assuming that the temperature dependence of $E_g/2-E_i$ is negligible (as the temperature at which measurement are made are not too high), the trap level may be calculated from the slope of ln $(J_0/T^{3/2})$ vs the $1/kT$ plot, however, the value of E_i needs to be known. The intrinsic energy level E_i was calculated using the relation[21]

$$E_i = \frac{E_c+E_v}{2} + \frac{3kT}{4} \ln \frac{m_h}{m_e}, \tag{4}$$

where m_h and m_e are the effective mass of the hole and electron and they are given by 0.64 and $0.077m_0$, respectively.[21] The value of E_i is estimated to be 0.71 eV. The trap level in the temperature range 300–375 K is found to be 0.71 eV (approximately mid-gap region).

For the temperatures below 270 K, the activation energy E_a is 0.28 eV, much less than half the band-gap energy suggesting a field emission process wherein the tunneling may take place through the thin interfacial layer.

In order to calculate the thickness of the interfacial layer, a tunneling factor: exp $(-0.26\ \chi^{1/2}\delta)$,[22,23] where χ is the difference in electron affinity between InP and the insulating layer, and δ the thickness of the insulating interfacial layer, is to be incorporated into the Richardson constant A^*. The tunneling probability depends upon δ, and δ itself is influenced strongly by the unknown value of χ. Precise values of χ are not known for the interfacial layer. However, for In_2O_3 and $InPO_4$ the value of χ is 0.2 and 1.1 eV, respectively.[24,25] δ is calculated for the range of value of χ from 0.2 to 1.2 eV. The corresponding interfacial layer thickness has been found to be between 25 and 35 Å, which is well within the tunneling range.

The presence of a thin interfacial layer also influence the C-V characteristics as explained in the following section.

C. *C-V* characteristics

Figure 7 shows the C^{-2} vs V_r plot for ITO/p-InP junction prepared at 340 °C with 5% tin. The relationship of capacitance and carrier concentration (N_A) may be written as[21]

$$\frac{dC^{-2}}{dV} = \frac{2}{q\epsilon_s N_A} \tag{5}$$

and

$$\frac{1}{C^2} = \frac{2}{q\epsilon_s N_A}(V_{bi}-V_r), \tag{6}$$

where ϵ_s is the permittivity of the semiconductor and V_{bi} is the built-in potential. N_A and V_{bi} are calculated from the

slope and the intercept of C^{-2}-V plot, respectively. V_{bi} was found to be 0.84 V, and the barrier height was calculated using the relation

$$\phi_b = V_{bi} + \frac{kT}{q} \ln\left(\frac{N_V}{N_A}\right) + \frac{kT}{q}. \tag{7}$$

The barrier height calculated from C-V measurements was 0.99 eV, which is a realistic value (earlier workers observed unrealistic value for sputtered and electron beam evaporated ITO/InP junctions).[4–6, 26]

The barrier height observed from C-V measurements is higher than that observed from the I-V data. The difference in the barrier heights is due to an insulating layer at the interface.

An insulating layer at the interface can modify the C-V characteristics if the potential across the interfacial layer changes with bias. The change in potential across the interfacial layer will modify Eq. (5) as[27]

$$\frac{dC^{-2}}{dV} = \frac{2(1+\alpha)}{q\epsilon_s N_A} \tag{8}$$

with $\alpha = qD_{sb}\delta/\epsilon_i$, where D_{sb} is the interface state density, δ is the insulating layer thickness, and ϵ_i is the permittivity of the insulator.

The deviation of V_0 (the diffusion potential measured from C^{-2}-V plot) from V_D, the actual diffusion potential can be written as[27]

$$V_0 = (1+\alpha)V_D + V_1^{1/2}V_D^{1/2} + \frac{V_1}{4(1+\alpha)}, \tag{9}$$

where $V_1 = 2q\epsilon_s N_D \delta^2 / \epsilon_i$. When δ is zero V_0 will be equal to V_D.

For MIS type of devices, the difference between the barrier heights ($\Delta\phi_b$) measured from the C-V and I-V measurements is given by[23,26,27]

$$\Delta\phi_b = \alpha V_D + V_1^{1/2}V_D^{1/2} + \frac{V_1}{4(1+\alpha)}. \tag{10}$$

In the present case $\Delta\phi_b$ is 0.38 eV. In order to account for this difference, the interfacial insulator thickness δ is to be of the order of 20–30 Å ($\epsilon_i \sim 6$ and $D_{sb} \sim 10^{13}$ cm^{-2} eV^{-1}) which is in good agreement with the value estimated from I-V measurements.

The C-V profiling carried out on these samples show that there is no change in carrier density up to 0.1 μm within the junction, hence the possibility of a homojunction (or surface modification of p-InP during junction fabrication as in the case of sputtered junctions) may be eliminated (figure not given).

III. CONCLUSIONS

In the present paper, XPS and transport studies have been carried out on spray pyrolytic grown ITO/p-InP junctions to characterize the interface and the transport mechanism across the junction. The XPS studies have confirmed an interfacial layer consisting of In_2O_3 and $InPO_4$; the thickness of the layer is estimated (from I-V and C-V measurements) to be of the order of 20–30 Å. The transport mechanism across the junction is analyzed and it is found that recombination at the depletion region is dominant above 270 K. The barrier height calculated from C-V has realistic value (0.99 eV) unlike the sputtered and electron beam evaporated ITO/p-InP junctions. The observed transport properties of sprayed ITO/p-InP have been explained on the basis of the MIS model.

ACKNOWLEDGMENTS

The authors would like to acknowledge Council of Scientific and Industrial Research, Government of India for financial help and Dr. C. S. Gopinath for useful discussions in analyzing the XPS data.

[1] M. B. Spitzer, C. J. Keavney, S. M. Vernon, and V. E. Haven, Appl. Phys. Lett. **51**, 363 (1987).
[2] M. Yamaguchi and K. Ando, J. Appl. Phys. **63**, 5555 (1988).
[3] M. Yamaguchi, C. Umera, and A. Yamamoto, J. Appl. Phys. **55**, 1429 (1984).
[4] X. Li, M. W. Wanlass, T. A. Gessert, K. A. Emery, and T. J. Coutts, Appl. Phys. Lett. **54**, 2674 (1989).
[5] T. J. Coutts, X. Wu, T. A. Gessert, and X. Li, J. Vac. Sci. Technol. A **6**, 1722 (1987).
[6] P. Manivannan and A. Subrahmanyam, J. Appl. Phys. **76**, 2912 (1994).
[7] M. Tsai, A. L. Fahrenbruch, and R. H. Bube, J. Appl. Phys. **51**, 2696 (1980).
[8] P. Sheldon, R. K. Ahrenkiel, R. Hayes, and P. E. Russell, Appl. Phys. Lett. **41**, 727 (1982).
[9] K. J. Bachmann, H. Schreiber, Jr., W. R. Sinclair, P. H. Schmidt, F. A. Thiel, E. G. Spencer, G. Pasteur, W. L. Feldmann, and K. Sree Harsha, J. Appl. Phys. **50**, 3441 (1979).
[10] A. Subrahmanyam, V. Vasu, P. Santana Raghavan, J. Kumar, and P. Ramasamy, Mater. Sci. Eng. B **14**, 365 (1992).
[11] V. Vasu, A. Subrahmanyam, J. Kumar, and P. Ramasamy, Semicond. Sci. Technol. **8**, 437 (1993).
[12] L. Gouskov, H. Luquet, J. Esta, and C. Gril, Solar Cell **5**, 51 (1981).
[13] G. Hollinger, E. Bergignal, J. Joseph, and Y. Robach, J. Vac. Sci. Technol. A **3**, 2082 (1985).
[14] D. T. Clark, X. Fok, G. G. Roberts, and R. W. Sykes, Thin Solid Films **70**, 261 (1980).
[15] A. Nelson, K. Geib, and C. W. Wilmson, J. Appl. Phys. **54**, 4134 (1983).
[16] N. Shibata and H. Ikoma, Jpn. J. Appl. Phys. **31**, 3976 (1992).
[17] E. H. Rhoderik and R. H. Williams, *Metal Semiconductor Contacts* (Clarendon, Oxford, 1988).
[18] N. Newman, M. van Schilfgaarde, and W. E. Spicer, Phys. Rev. B **35**, 6398 (1987).
[19] A. Yu and E. H. Snow, J. Appl. Phys. **39**, 3008 (1968).
[20] M. Wolf, G. T. Noel, and R. J. Stirm, IEEE Trans. Electron Devices **ED-24**, 419 (1969).
[21] S. M. Sze, *Physics of Semiconductor Devices* (Wiley, New York, 1969).
[22] C. R. Crowell, Solid-State Electron. **20**, 171 (1977).
[23] A. K. Srivastava, B. M. Arora, and S. Guha, Solid-State Electron. **24**, 185 (1981).
[24] S. G. Goodnick, T. Hwang, and C. W. Wilmsen, Appl. Phys. Lett. **44**, 453 (1984).
[25] L. G. Meiners, J. Electrochem. Soc. **133**, 372 (1986).
[26] H. Thomas and J. K. Luo, J. Appl. Phys. **73**, 3058 (1993).
[27] H. C. Card and E. H. Rhoderick, J. Phys. D **4**, 1586 (1971).